Journal of Alloys and Compounds 509 (2011) 3855–3858

Contents lists available at ScienceDirect

Journal of Alloys and Compounds

journal homepage: www.elsevier.com/locate/jallcom

Cerium concentration and temperature dependence of the luminescence of $Lu_2Si_2O_7$:Ce scintillator

He Feng[a,b], Dongzhou Ding[a], Huanying Li[a], Sheng Lu[a], Shangke Pan[a], Xiaofeng Chen[a], Guohao Ren[a,*]

[a] Shanghai Institute of Ceramics, Chinese Academy of Sciences, 215 Chengbei Road, Jiading, Shanghai 201800, People's Republic of China
[b] Department of Materials Science and Opto-Electronic Engineering, National Sun Yat-Sen University, Kaohsiung 804, Taiwan, ROC

ARTICLE INFO

Article history:
Received 10 May 2010
Received in revised form
16 December 2010
Accepted 17 December 2010
Available online 24 December 2010

Keywords:
LPS:Ce
Cerium concentration dependence
Temperature dependence
Scintillation properties

ABSTRACT

The crystals of $(Lu_{1-x}Ce_x)_2Si_2O_7$ (LPS) (x = 0.003, 0.005, 0.0075, 0.01 and 0.013) are grown by Czochralski (Cz) method. The scintillation and optical properties of these LPS:Ce crystals were studied and compared systematically, mainly focused on the absorption, photoluminescence (PL) and photoluminescence excitation (PLE) and decay time. It is found that the self absorption of LPS:Ce is increased as the cerium doping concentration increases; the PLE curves of LPS:Ce samples are influenced by the both cerium doping concentrations and sample thickness. Specially, thicker and higher cerium doped LPS:Ce, i.e. the stronger self absorption, will lead to incomplete PLE curves. The temperature dependence of luminescence of LPS:0.3%Ce, including the decay time, PLE and PL properties, is investigated.

1. Introduction

Cerium-doped lutetium pyrosilicate $Lu_2Si_2O_7$:Ce (LPS:Ce) is a high performance scintillator found in 2000 [1], which exhibits outstanding scintillation properties: high light yield (26,000 photons/MeV), short decay time (38 ns) without observable afterglow and high density (6.2 g/cm^3). So it is a good candidate scintillator used for the X-ray and γ-ray detection devices due to its outstanding scintillation and physical performance. LPS has the thortveitite structure, with monoclinic symmetry, space group C2/m and only one single crystallographic site for lutetium ions [2]. The LPS:Ce scintillator can be used for oil-well logging because of its high temperature light yield (up to 450 K) [3]. Some meaningful research results have been obtained such as the energy level scheme [4] and EPR investigation of Ce^{3+} [5] in LPS. The crystal growth and annealing effects study on LPS:Ce scintillation crystal have also been reported in Refs. [6,7].

Generally speaking, the cerium concentration and temperature play important impact on the scintillation performance of cerium doped luminescent materials, such as photoluminescence (PL), photoluminescence excitation (PLE), luminescence efficiency and decay time properties [8–13]. So it is meaningful to study the influence of cerium concentration and temperature on the optical and scintillation properties of cerium-doped scintillators. The temperature dependence research of LPS:Ce has been carried out by Pidol et al. [3,14,15]. Up to now, there has been no paper published related to the cerium doping concentration effect on LPS:Ce.

In order to fill up this research gap, the cerium concentration effect on the scintillation properties of LPS:Ce, including absorption, decay time, PL and PLE properties were analyzed and discussed systematically in this paper. At the meantime, the temperature dependence of LPS:0.3%Ce is investigated at different temperature within the 77–500 K range, focused on the PLE, PL and decay time properties.

2. Experimental

All the LPS:Ce crystals studied in this paper were grown by the Czochralski (Cz) method. The starting powder materials are Lu_2O_3, SiO_2 and CeO_2 with 4N purity. The preparation and crystal growth procedures are as follows: these starting materials were dried at 200 °C for 10 h under air to drive away the moisture and weighted and mixed with stoichiometry of $(Lu_{1-x}Ce_x)_2Si_2O_7$ (x = 0.003, 0.005, 0.0075, 0.01 and 0.013, unit:molar concentration). Then these materials were shaped into cylinder rods under 200 MPa isostatic press. These rods were sintered at 1500 °C in air for 10 h in order to obtain polycrystalline charge of LPS. The crystal growth was carried out in an induction heating crystal growth furnace under high pure argon atmosphere. These sintered rods were loaded into iridium crucible with 50 mm in diameter and 30 mm in height. Single pure LPS crystal seeds were used. The rotation and pulling rates were 5 rpm and 0.5 mm/h, respectively. The size of crystal boules obtained was about 15 mm in diameter and 25 mm in length, through an automatic up metage control system developed by Cyberstar Corporation. Each sample was cut and polished from the neck position of boule to make sure the comparison of

* Corresponding author at: Shanghai Institute of Ceramics, Chinese Academy of Sciences, 215 Chengbei Road, Jiading, Shanghai 201800, People's Republic of China. Tel.: +86 21 6998 7740; fax: +86 21 5992 7184.
E-mail address: rgh@mail.sic.ac.cn (G. Ren).

0925-8388/$ – see front matter © 2010 Elsevier B.V. All rights reserved.
doi:10.1016/j.jallcom.2010.12.124

the scintillation properties is under the same condition. All obtained samples are colorless and transparent.

Optical absorption spectra were measured by using a Shimadzu UV-2501 PC spectrophotometer. The decay time, PL and PLE curves at different temperature were recorded on the Edinburgh FLS-920 steady state and time resolved fluorescence spectrometers. In the PL and PLE curves measurement procedure, the 450W Xe arc lamp was used as the excitation source. The excitation and emission slit are both 0.25 nm and the step is 1 nm. In the decay time measurement, a nanosecond flashlamp (900 nF) is used as the excitation source. The time-correlated single photon counting technology was adopted to record fluorescence decay curve. The real decay time data was obtained through the reconvolution fit, deducting the instrument response function and the noise influence.

3. Results and discussion

3.1. The absorption spectra of LPS:Ce crystals

Fig. 1 shows the absorption spectra of LPS:Ce samples with 2 mm thickness. It is shown that the absorption spectra of the five samples are similar; the absorption between 200 and 380 nm is regarded as the role of Ce^{3+} ions. Two main absorption peaks center at 305 and 350 nm, corresponding to the Ce^{3+} electron transition from the 4f ground state to the two lowest 5d sublevels [16]. The absorption below 250 nm is attributed to the 4f ground state to the higher 5d sublevels [17].

Of course, the variation of the cerium doping concentration will bring change to the absorption spectra. The spectra in the 350–380 nm range are magnified in the inset (i). From the inset, we can see that the absorption edges of the LPS:Ce samples move towards longer wavelength direction with increasing cerium doping concentration. This phenomenon means that the self absorption increases with the cerium doping concentration increase. As we know, the integral value of the absorption curve between 250 and 380 nm is a convincible index of cerium ion concentration. From the integral values, we can compare the actual cerium ion concentrations on the lutetium site in different LPS crystals, as shown in inset (ii). When cerium doping concentration is 0.3%, the actual cerium is at the minimum level. When the cerium doping concentration is below 0.75%, the actual cerium concentration gradually increases with the increasing cerium doping concentration. When the cerium doping concentration is over 0.75%, the actual cerium concentration only slightly increases as the doping concentration increases, arriving at the maximum at 1.3% cerium doping concentration. The phenomenon means that the doping concentration under 0.75%

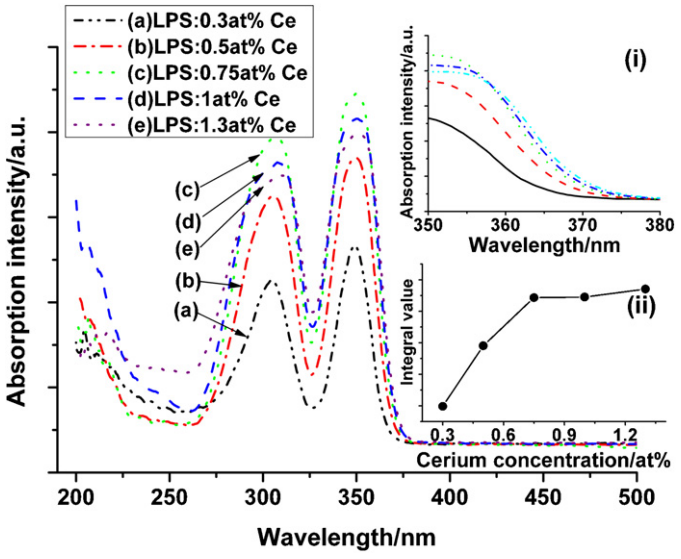

Fig. 1. The absorption spectra of LPS:Ce with different cerium doping concentrations.

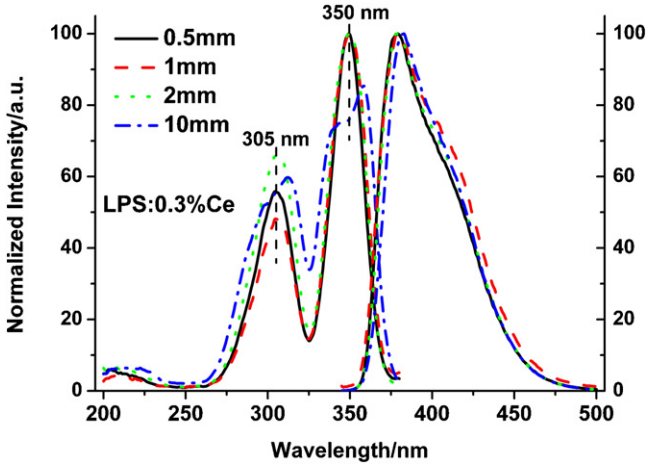

Fig. 2. The PLE and PL curves of LPS:0.3%Ce with different sample thickness (0.5, 1.0, 2.0 and 10 mm)

should be preferred. Considering that there is only one single crystallographic site for lutetium ions [2] and ions radius of Lu^{3+} in LPS is much smaller than that of Ce^{3+} (Ce^{3+}:1.034 Å, Lu^{3+}:0.848 Å) [18], this is a reasonable phenomenon.

3.2. PLE and PL spectra of LPS:Ce samples

Fig. 2 shows the PLE and PL curves of LPS:0.3%Ce with different four sample thickness: 0.5, 1, 2 and 10 mm, respectively. All samples are located at the same position to make sure that the same condition is kept during the measurement process. The PLE and PL curves of the former three samples are normalized. It is presented that the PLE peaks of them are similar with each other: there are two PLE peaks peaking at 305 and 350 nm, corresponding to the electron transition from 4f ground to 5d transition of Ce^{3+}. It is noticed that the PLE curve of 10 mm sample is obviously different from that of the other three thinner samples: the two PLE peaks are incomplete. Because the sample thickness is the only change condition during the measurement, the incomplete PLE curve must be induced by the sample thickness. Considering that the self-absorption increases as the sample thickness increase in cerium doped scintillator [19], this phenomenon is attributed to the strong absorption of the thick sample. It is concluded that sample thickness is one of the factors which should be taken into consideration in the PLE curve measurement process. If possible, relative thin sample (may be thinner than 1 mm) is preferred to avoid the incomplete PLE curves.

Fig. 3 displays the PLE and PL spectra of LPS:Ce crystals with the five different cerium doping concentrations. It is shown that all the PLE curves are composed of two PLE peaks centering at about 305 and 350 nm. As the cerium concentration increases, the relative intensity of 305 nm peak also increases gradually. Let's pay attention to the PLE curve of LPS:1.3%Ce, it is obvious that the PLE curve is also incomplete as that of the LPS:0.3%Ce with 2 mm thickness. As discussed above (the higher cerium concentration, the stronger absorption intensity), we can also attribute this phenomenon to the absorption increase, especially around the PLE peaks.

Through Gaussian fitting, all of the PL curves can be decomposed into two peaks centering nearly at 376 and 400 nm, respectively, corresponding to the Ce^{3+} electron transition from lowest 5d level to the two spin–orbit split 4f sublevels, $^2F_{5/2}$ and $^2F_{7/2}$. With the increasing cerium concentration or increasing sample thickness, the PL curves move towards the longer wavelength direction. This phenomenon is attributed to the red shift of absorption edge. Obviously, the PL curves are not so sensitive to the cerium doping concentration and sample thickness as the PLE curves do.

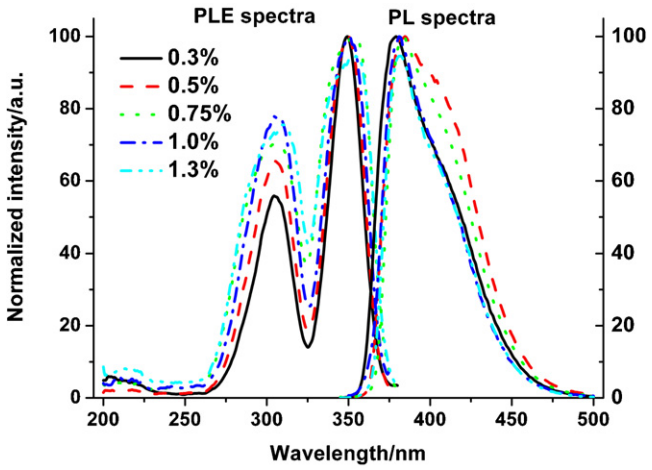

Fig. 3. The PLE and PL spectra of LPS:Ce crystals with different cerium doping concentrations.

Fig. 4 shows the PLE (a) and PL (b) spectra of LPS:0.3%Ce from 77 K to 500 K. Under 77 K, there are two PLE peaks centering at 303 nm and 350 nm, respectively, called peak 1 and peak 2 for short. The intensity ratio between the two peaks (peak 1 relative to peak 2) is about 1.12. As the temperature increases, three obvious phenomena can be observed: (1) the intensity ratio decreases gradually (from 1.12 at 77 K to 0.72 at 400 K); (2) both peak 1 and peak 2 are broadened; (3) the peak 1 moves towards the longer wavelength direction, while the peak 2 locates at 350 nm up to 450 K, only moving to 353 nm at 500 K. Phenomenon (1) can be explained through the thermalization of Ce^{3+} 5d electrons on different sublevels. In LPS host, five 5d sublevels of Ce^{3+} are located above the 4f ground level at 3.55 eV (5d(1)), 4.1 eV (5d(2)), 5.1 eV (5d(3)), 5.95 eV (5d(4)) and 6.7 eV (5d(5)), respectively according to Pidol's paper [4]. The peak 1 is corresponding to the electron transition from 4f ground level to 5d(2) sublevel; peak 2 is corresponding to the electron transition from 4f ground level to 5d(1) sublevel. As the temperature increases, the 5d electrons of Ce^{3+} will be thermalized into conduction band [20]. Now that the energy level position of 5d(2) sublevel is higher than that of 5d(1) sublevel, the electron on 5d(2) sublevel will firstly thermalize into conduction band when temperature increases. Those thermalized 5d electrons will not give the 5d–4f Ce^{3+} emission, leading to the decrease of excitation intensity of peak 1 and the ratio between the two peaks. Besides above problem, the increased temperature will also intensify the electron vibration on 5d and 4f levels, resulting in the decrease of energy gap between ground 4f level top and 5d(2) sublevel bottom, which is corresponding to the red-shift of PLE peaks. At the meantime, the intensified electron vibration slightly increases the energy level difference between the 4f level bottom and the 5d(2) sublevel top. So the PLE curves will also broaden towards the shorter wavelength direction, as seen in Fig. 4(a). As for peak 2, because it is corresponding to the electron transition from 4f to the lowest 5d(1) sublevel, which is shielded by 5d(2) sublevel, the thermal impact on it is weaker than peak 1. As temperature increases, it mainly presents a slight thermal broadening effect. Its peak position stays stable up to 450 K, and just moves to 353 nm at 500 K.

Fig. 4(b) shows the PL spectra of LPS:0.3%Ce crystal from 77 to 500 K (normalized intensity). At 77 K, the PL curve can be fitted into two peaks centering at 376 and 404 nm, respectively, as seen the inset (i). As temperature increases, the curves gradually broaden and move to the longer wavelength direction. The peak position of PL curves gradually moves from 377 nm at 77 K to 391 nm at 500 K. The PL curve at 500 K can be fitted into two peaks, peaking at 385 and 410 nm, respectively, as seen in inset (ii). These fitted

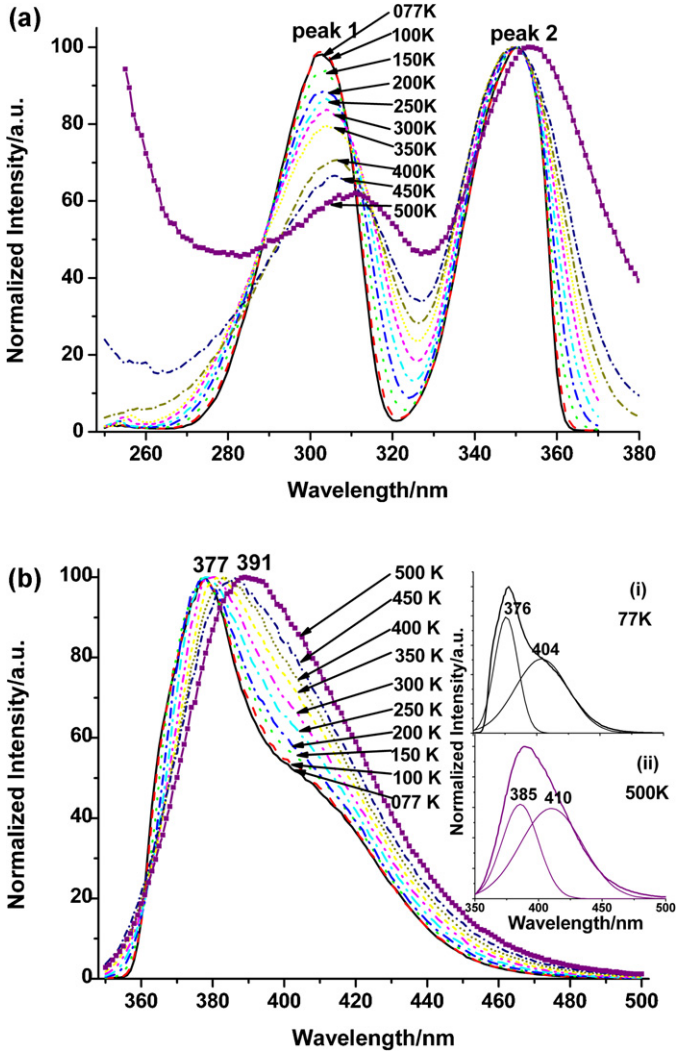

Fig. 4. The PLE (a) and PL (b) spectra of LPS:0.3%Ce from 77 K to 500 K (77–250 K:λ_{ex} = 303 nm, λ_{em} = 378 nm; 300 K: λ_{ex} = 304 nm, λ_{em} = 380 nm; 350 K: λ_{ex} = 304 nm, λ_{em} = 383 nm; 400 K: λ_{ex} = 307 nm, λ_{em} = 383 nm; 450 K: λ_{ex} = 307 nm, λ_{em} = 386 nm; 500 K: λ_{ex} = 311 nm, λ_{em} = 389 nm).

peaks are corresponding to the electron transition from lowest 5d sublevel 5d(1) to two 4f sublevels, $^2F_{5/2}$ and $^2F_{7/2}$, respectively [21]. So these tendencies of PL curves can be attributed to the gradually increasing thermalization and vibration of the electrons on 5d(1) sublevel as the temperature increases. Meanwhile, the overlap part between PL and PLE curves will also gradually increases as the PLE and PL curves broaden. It means that the self absorption of LPS:Ce will increase as the temperature increases [22,23].

3.3. The decay time curves

At this part we will discuss the cerium concentration and temperature dependence of decay time. Fig. 5 shows the decay time under different cerium doping concentrations of LPS:Ce. It is noticed that all five curves of LPS:Ce can be fitted through the single exponential function, so only the decay curve of LPS:0.3%Ce is shown in the inset as an example. Through the single exponential fit, the decay time of LPS:0.3%Ce is 36 ns under excitation at 350 nm and emission at 380 nm. As we can see from the figure, the decay time of the samples maintains between 36 and 41 ns. This phenomenon means that the concentration quenching effect does not occur below the 1.3% doping concentration.

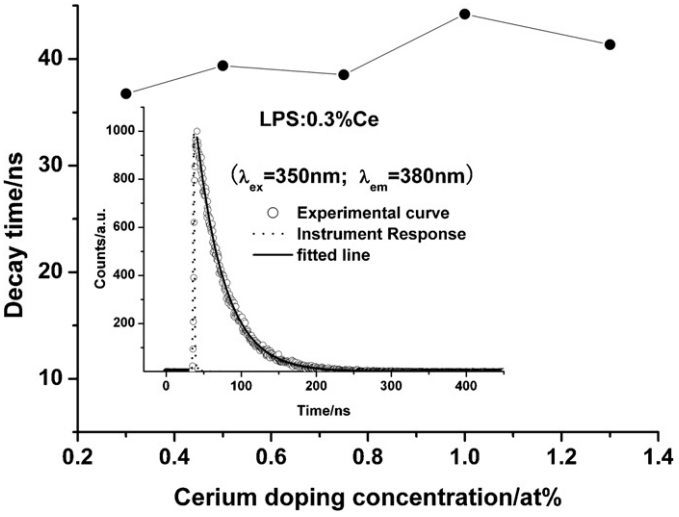

Fig. 5. The decay curves of LPS:Ce with different cerium concentrations (the open dots are the decay curve, small dots are instrument response, line is the fitted line).

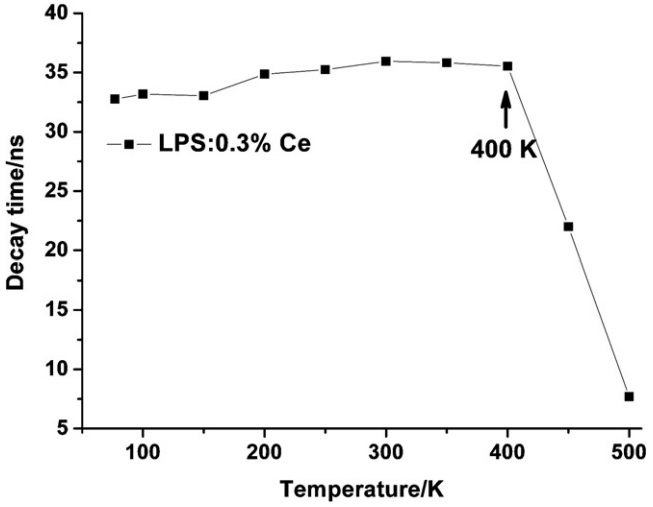

Fig. 6. The decay time of LPS:0.3%Ce under different temperature.

Fig. 6 displays the decay time of LPS:0.3%Ce under different temperatures, all the decay time curves show single exponent fitting characteristic. From 77 to 500 K, the curve presents two district tendencies. The dividing temperature point locates at about 400 K. Under 400 K, the decay time increases slightly as the temperature is raised. Above this temperature point, the decay time begins to decrease sharply, when the temperature comes to 500 K, the decay time of LPS:Ce is only 9 ns. From Fig. 4, we already know that the self absorption of LPS:Ce will increase gradually as the temperature increases. The increasing absorption will lead to the increasing delayed Ce^{3+} emission [14]. So it is reasonably observed that the decay time slight increases below 400 K. Although the self absorption still increases above 400 K, the decay time sharply shortens above this point. This is attributed to the thermal ionization of Ce^{3+} 5d(1) electron into conduction band [14].

4. Conclusions

Cerium-doped lutetium pyrosilicate $(Lu_{1-x}Ce_x)_2Si_2O_7$:Ce (LPS) (x = 0.003, 0.005, 0.0075, 0.01, 0.013) crystals are grown by Czochralski method. The scintillation and optical properties of LPS:Ce crystals with different cerium doping concentrations were studied and compared systematically, mainly focused on the absorption, photoluminescence and photoluminescence excitation and decay time. It is found that the self absorption of LPS:Ce increases as the increase of cerium doping concentration and temperature; the PLE curves of LPS:Ce samples are influenced by the both cerium doping concentrations and sample thickness; the concentration quenching effect does not occur in the investigated cerium doping range.

Acknowledgement

This work was supported by the National Natural Science Foundation of China (Grant No. 50902145), the Natural Science Foundation of Shanghai (Grant No. 09ZR1435800) and the Knowledge Innovation Program of the Chinese Academy of Sciences (Grant No. SCX200701). This document was prepared as an account of work sponsored by China. Professor Wang Shaohua and Chen Junfeng did the main measurement work presented in this paper.

References

[1] D. Pauwels, N. le Masson, B. Vianan, A. Kahn-Harari, E.V.D. van Loef, P. Dorenbos, C.W.E. van Eijk, IEEE Trans. Nucl. Sci. 47 (2000) 1787.
[2] F. Bretheau-Raynal, M. Lance, P. Charpin, J. Appl. Cryst. 14 (1981) 349.
[3] L. Pidol, A. Kahn-Harari, B. Vianan, B. Ferrand, P. Dorenbos, J.T.M. de Hass, C.W.E. van Eijk, E. Virey, J. Phys.: Condens. Matter 15 (2003) 2091.
[4] L. Pidol, B. Viana, A. Kahn-Harari, A. Galtayries, A. Bessiere, P. Dorenbos, J. Appl. Phys. 95 (2004) 7731.
[5] L. Pidol, O. Guillot-Noël, A. Kahn-Harari, B. Viana, D. Pelenc, D. Gourier, J. Phys. Chem. Solids 67 (2006) 643.
[6] P. Szupryczynski, C.L. Melcher, M.A. Spurrier, A.A. Carey, M.P. Maskarinec, B. Chakoumakos, C. Rawn, R. Nutt, Proc. IEEE Nucl. Sci. Sympos. Conf. 3 (2005) 1310.
[7] H. Feng, D.Z. Ding, H.Y. Li, S. Lu, S.K. Pan, X.F. Chen, G.H. Ren, J. Appl. Phys. 103 (2008) 083109.
[8] A. Fukabori, T. Yanagida, F. Moretti, Y. Yokota, R. Shimura, S. Maeo, J. Pejchal, K. Kamada, A. Yoshikawa, Radiat. Meas. 45 (2010) 453.
[9] T. Shalapska, G. Stryganyuk, A. Gektin, P. Demchenko, A. Voloshinovskii, P. Dorenbos, J. Phys.: Condens. Matter 21 (2010) 485503.
[10] H. Feng, V. Jary, E. Mihokova, D.Z. Ding, M. Nikl, G.H. Ren, H.Y. Li, S.K. Pan, A. Beitlerova, R. Kucerkova, J. Appl. Phys. 108 (2010) 033519.
[11] Y. Toriyabe, E. Yoshida, J. Kasagi, Nucl. Instrum. Meth. A 611 (2009) 69.
[12] H. Yokota, M. Yoshida, H. Ishibashi, T. Yano, H. Yamamoto, S. Kikkawa, J. Alloys Compd. 495 (2010) 162.
[13] X.M. Zhang, B. Park, N. Choi, J. Kim, G.C. Kim, J.H. Yoo, Mater. Lett. 63 (2009) 700.
[14] L. Pidol, B. Viana, A. Galtayries, P. Dorenbos, Phys. Rev. B 72 (2005) 125110.
[15] L. Pidol, A. Kahn-Harari, B. Viana, E. Virey, B. Ferrand, P. Dorenbos, J.T.M. de Haas, C.W.E. van Eijk, IEEE Trans. Nucl. Sci. 51 (2004) 1084.
[16] G. Blasse, B.C. Grabmaier, Luminescent Materials, Springer, Berlin, 1994.
[17] C.F. Yan, G.J. Zhao, Y. Hang, L.H. Zhang, J. Xu, J. Cryst. Growth 281 (2005) 411.
[18] R.D. Shannon, C.T. Prewitt, Acta Crystallogr. B 25 (1969) 925.
[19] D.H. Cao, Y.J. Li, G.J. Zhao, J.Y. Chen, Q. Dong, Y.C. Ding, Acta Optica Sinica 29 (2009) 3463 (in Chinese).
[20] L.J. Lyu, D.S. Hamilaton, J. Luminesc. 48–49 (1991) 251.
[21] Y. Pei, X.F. Chen, L.S. Qin, D.M. Yao, G.H. Ren, Chin. Phys. 15 (2006) 2756.
[22] A.J. Wojtowicz, E. Berman, A. Lempicki, IEEE Trans. Nucl. Sci. 39 (1992) 1542.
[23] W. Drozdowski, A.J. Wojtowicz, Nucl. Instrum. Meth. A 486 (2002) 412.